A Novel Peak Detection Algorithm for Use in the Study of Machining Chip Segmentation

Eric Whitenton, Robert Ivester, and Jarred Heigel
Manufacturing Engineering Laboratory
National Institute of Standards and Technology
Gaithersburg, MD 20899, USA
Eric.Whitenton@Nist.Gov

Abstract

The study of how metal deforms and flows as parts are machined yields important insights into the metal cutting process. Improvements in high-speed digital imaging and image processing software promise to improve our understanding of the tool-workpiece interface and verify the accuracy of finite element modeling simulations. This will ultimately enable industry to improve machining processes and make parts faster at less cost. This report describes the design and results of an automated system to estimate chip segmentation frequency. High-speed images of machining chips are combined with displacement vector mapping and processing. As part of the displacement vector map processing, a novel peak detection algorithm using an inflection list was developed which minimizes a priori assumptions and yields information used in sensitivity analysis. However, further work is needed before an uncertainty analysis may be completed.

Keywords: machining chip segmentation, high-speed video, vector map, peak detection.

1 INTRODUCTION

When metal parts are machined, the unwanted pieces of removed material are called machining chips. Studying how metal is deformed and flows as these chips are created yields important insights into the metal cutting process, which promise to improve and verify the accuracy of finite element modeling simulations of this process. These simulations are an important tool for process optimization, ultimately allowing industry to make parts faster, better, and at less cost.

There are two basic types of chips, **continuous** chips and **segmented** chips. Continuous chips are long and ribbon-like in shape and can become entangled in the machining equipment. Segmented chips have a characteristic saw tooth shape and tend to break up into small pieces that are much easier to control than continuous chips. This makes the manipulation of machining conditions to encourage segmented chip formation a topic of great interest to the machining community.

The reason segmented chips do not become long ribbons is that the metal in the gaps between the segments is brittle and breaks easily. Breakage occurs when the chip curls back into the workpiece, causing a force to be applied to the brittle gap. While most of these gaps do not break, enough of them do to keep the chip from getting very long.

Using photomicrographs like the one in Figure 1, the final size and shape of the segments can be measured after the machining has finished [2]. Even within the same chip, the segments sizes and shapes vary widely. However, producing these photomicrographs is labor and time intensive. Thus, studying the size and shapes of segments generally involves small sample sizes, which limits researchers to the study of an "average" segment with relatively high uncertainties. Additionally, small sample sizes make characterization of segment formation by statistical or dynamical calculations (such as computing the dimension of an attractor [1]) difficult.
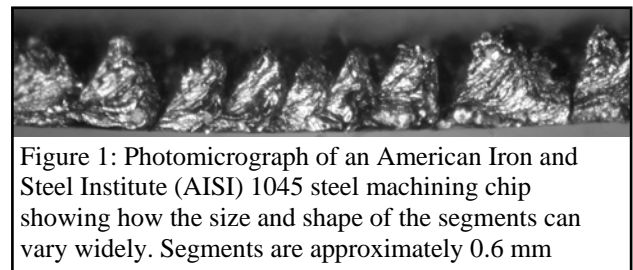

Figure 1: Photomicrograph of an American Iron and Steel Institute (AISI) 1045 steel machining chip showing how the size and shape of the segments can vary widely. Segments are approximately 0.6 mm

The machining community interprets the final size and shape of the chips to infer how the metal flowed and deformed during machining. The validity of these inferences are a matter of debate. Fortunately, recent advances in high-speed digital imaging technology and image processing software make possible the direct observation and characterization of metal cutting

processes [3, 11]. This paper will outline the use of this equipment to automatically estimate chip segmentation frequency, the rate at which segments form. A novel peak detection algorithm used in this application will be described in detail.

2 PHYSICAL MEANING OF THE DATA

Figure 2 shows the experimental setup. The edge of an American Iron and Steel Institute (AISI) 1045 steel disk is machined and 128 pixel x 128 pixel images of the tool workpiece interface are captured using a high-speed camera at 60 000 frames per second.
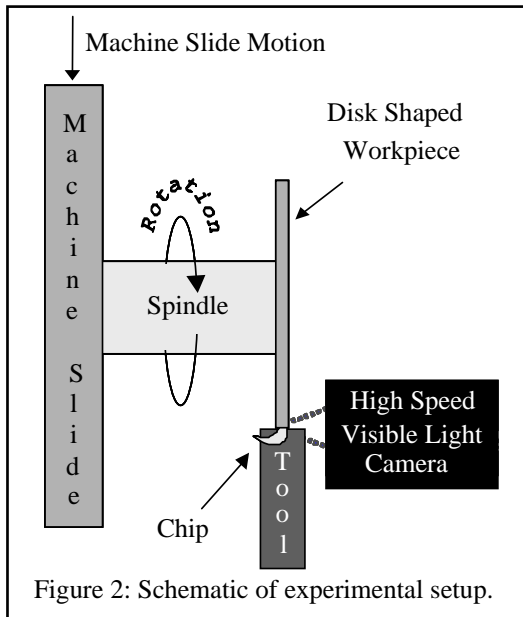
Figure 3 shows a typical image. Movies of cutting experiments will often have 20 000 to 100 000 images to process. Special "strain mapping" software [4] compares adjacent frames of the movie using correlation functions and computes a series of displacement vector maps describing how the features in the images have moved from one frame to the next. An example displacement vector map is shown in Figure 4. These displacement vectors can provide valuable information to the machining community. For example, shear strain can be computed and compared to the strain predicted by finite element models.

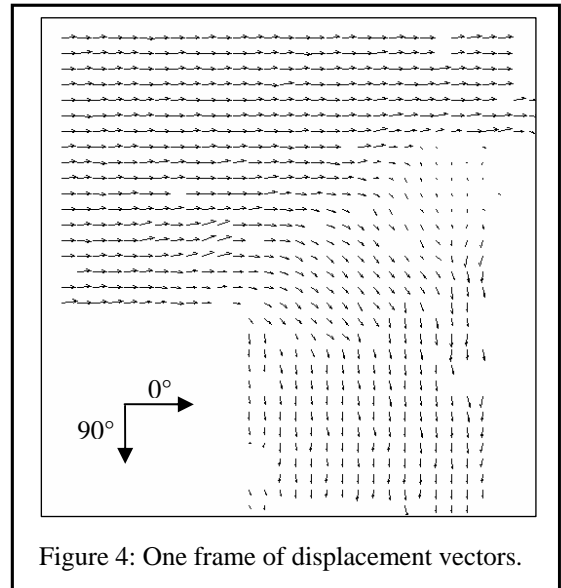Figure 4: One frame of displacement vectors.

Figure 2: Schematic of experimental setup.

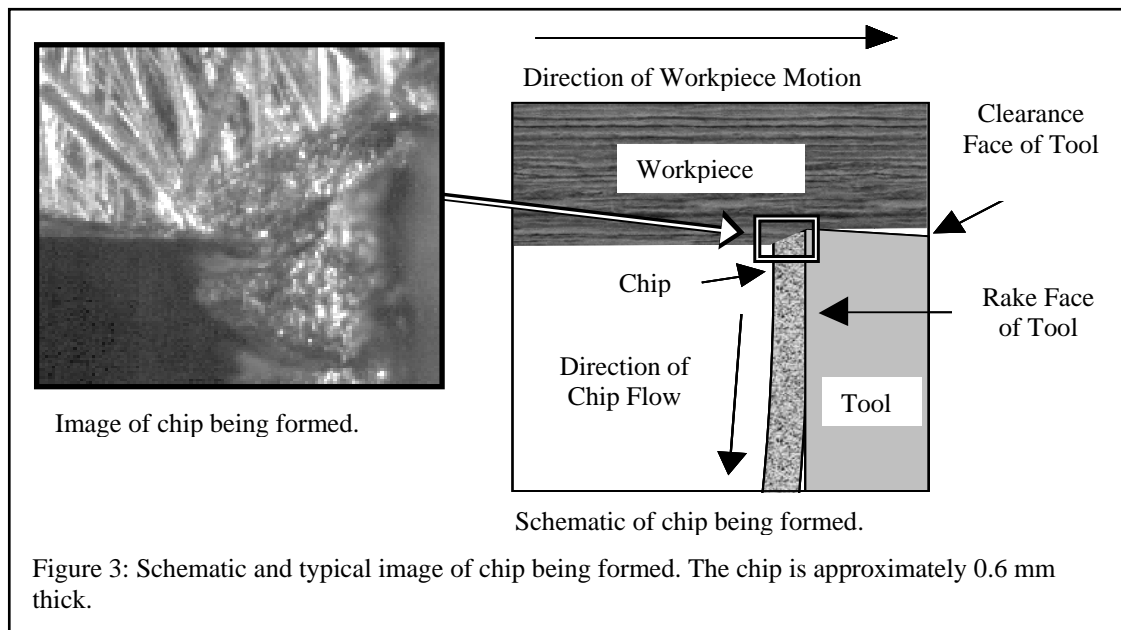Image of chip being formed.

Schematic of chip being formed.

Figure 3: Schematic and typical image of chip being formed. The chip is approximately 0.6 mm thick.

In order for the strain maps to be accurate, the images must be lit properly so that surface features are clearly visible. Also, spurious reflections which might confuse the strain mapping software should be minimized. A visual inspection of the images in the movies confirmed that these conditions were met. In addition, the frame rate should be high enough to both avoid Nyquist Frequency issues and allow the vector mapping software to yield accurate results. If the change from one frame to the next is too large, the vector mapping software will have difficulty computing accurate displacement vectors. This issue is revisited later in this paper.

One important statistic of interest is the rate at which segments are formed during cutting, called the **chip segmentation frequency**. To determine this frequency, traditional pattern matching could be performed on the original images to determine when a segment forms. One could design a template to detect the gaps between segments. Whenever a new gap appears and is detected by the pattern matching filter, a segment has formed. If the movie is processed and the number of frames between each segment formation is tallied, segmentation frequency can be computed. Note that when detecting gaps between segments, one is relying on the gaps being large enough to be visible. With this method, the pattern matching filter is detecting the *results* of the flow of material as it deforms. However, if displacement vectors are used instead, the *flow* of material is directly assessed and measured. This enables detection of segments that may be missed by traditional pattern matching on the images.

For the machining conditions currently under study, a consistent series of events is observed as segments form. As material approaches the tool from left to right, the material destined to become a chip comes in contact with the tool, stops, rotates, and starts to travel down along the rake face of the tool. Displacement vectors near the tool exhibit the following repeating cycle: Start at about 0° (left to right), rotate toward 90° as the material stops and rotates, and become 90° (pointing down) as the material travels along the rake face. This process repeats over and over – regardless of whether or not a visible gap forms. Figures 4 and 5 occurred during the rotate portion of the process.

To detect the segmentation events, a map of the vector angle minus 45° is computed. Shown in Figure 5, areas where the vectors are near 45° have a value near zero and are turned white. Areas with vectors near 0° or 90° have values near –45° or +45° and are turned black. If one considers only the vectors in the portion of the image where the rotation occurs and selects n vectors in that area, the following measure is used:

$$V = \frac{\sum_{j=1}^{n} |\theta_j - 45°|}{n}, \qquad (1)$$

where θ is the vector angle and V is a measure of how much a "typical" vector deviates from 45°. As segments form, the value of V oscillates between a minimum when most of the vectors are near 45°, and a maximum when most are either at 0° or 90°. V is, in effect, a matching function measuring how well the vectors match a template vector of 45°.
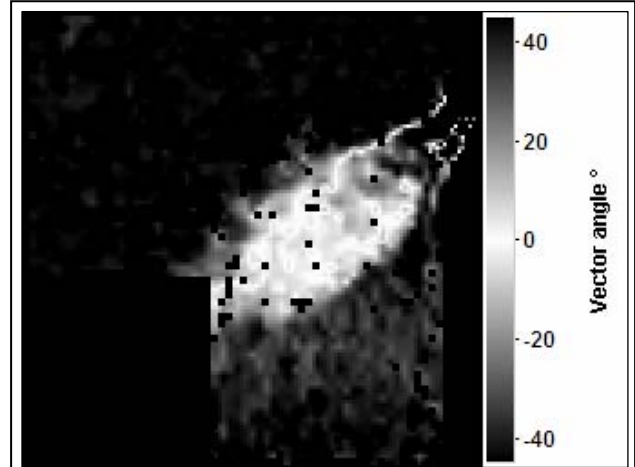

Figure 5: An image of the difference between the angle of the vectors in Figure 4 and 45°.

An example of V as a function of time is shown in Figure 6. Note that the amplitudes of the peaks and valleys change over time. Included in the figure are diamonds marking the "larger" peaks, and squares marking an estimation of when new segments form based on a visual examination of the movie.

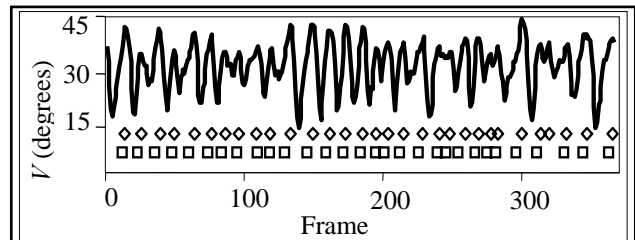Figure 6: V as a function of frame number. Larger peaks in V and visual estimations of when segments form are marked with diamonds and squares, respectively.

The agreement between the larger peaks and the human estimation is very good, with only one disagreement near frame 320, where the peaks indicated the formation of a segment that the examiner did not see. Upon re-examination of the movie, it was noticed that

there was, in fact, a small segment missed by the examiner. The human examiner relies primarily on gaps between segments to determine when segments are formed, similar to the traditional pattern matching method. This contrasts to using vector maps, where the material flow is used as the criterion. If two segments do not form a visible gap, the human operator might miss a segment which the vector algorithm would detect. An example is shown in Figure 7. This issue will be revisited later in the paper.
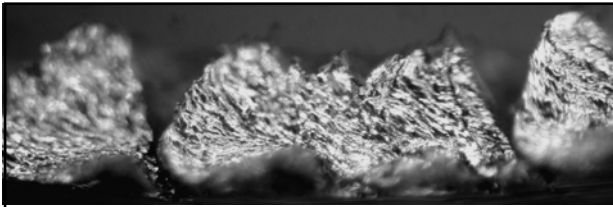

Figure 7: Photomicrograph of a large segment sandwiched between two smaller segments. It is unclear if the large segment is actually one segment, or several smaller segments compressed together. Segments are approximately 0.6 mm high.

Figure 6 shows "large" peaks indicating segment formation and "small" peaks which do not. There are several sources of these "small" peaks such as vibration of the tool, minor disturbances in the flow of the material, and errors in the calculated displacement vectors. A peak detection algorithm is required for separating "large," significant peaks indicating a segment formation and "small" peaks caused by other phenomenon.

3   SELECTING AND DESIGNING PEAK DETECTION ALGORITHMS

There are many peak detection algorithms available [5-9], each with a strategy for differentiating between significant (generally large) peaks to accept, and insignificant (generally small) peaks to ignore. Each algorithm makes assumptions as to the nature of either the data or the peaks in the data. Perhaps the most common assumption is that the data is stationary. **Stationary** data has the property that the probability distribution of the data at a fixed time is the same for all times. Parameters such as mean and variance do not change over time. If the data is non-stationary, and a peak detection algorithm is used which assumes stationary data, then assumptions must be made as to an appropriate **de-trending** function to transform the data into stationary data.

Another common assumption is that the significant peaks should have a width greater than some minimum, implying that insignificant peaks have a width smaller than the significant peaks. Some algorithms assume peaks occur at regular intervals, as when detecting harmonic frequencies in a Fourier transform. Some assume a fixed

threshold, while others dynamically compute new threshold values based on an analysis of the data in the local neighborhood.

The following assumptions are made regarding V in Equation 1:
- One must assume that there is some characteristic which separates important peaks from the unimportant ones. We chose to assume that the unimportant peaks are smaller in amplitude (not necessarily in width) than important ones. This seems to be a reasonable assumption given the known error sources. For example, apparent motion due to camera vibration is very small compared to the motion of the material in the images. Also, since V is the average behavior of n vectors, even if one or two vectors occasionally had large errors, their effect would be reduced by averaging.
- It is acceptable to determine each peak location to the nearest frame number (integer X). To interpolate between frames, one must assume an interpolation model such as a line or parabola. However, we lack a physically based reason to intelligently select any model.

Analysis of data from machining experiments yields the following desirable characteristics of an appropriate algorithm:
- Allow for non-stationary data without assuming a de-trending function. As cutting conditions change, the local average of V can slowly wander, even within the same cut.
- Make as few assumptions regarding the nature of the underlying data as possible. Specifically, no assumptions should be made regarding peak width because the peak width is strongly related to segmentation frequency, which is what we are trying to measure.
- Produce information to aid in sensitivity analysis, which determines how sensitive errors in the computed segmentation frequency are to errors in selecting the "correct" threshold value. This may be used to determine the uncertainty [10] of the estimated segmentation frequency.
- We desire to perform statistical and dynamical analysis on the data, which requires large data sets. Generally, over 20 000 frames will be processed per test. In addition, the peak detection algorithm will probably need to scan the data repeatedly, not just once. Thus, computational efficiency is important.

Unfortunately, none of the "off-the-shelf" peak detection algorithms met all of the desired assumptions and characteristics.

4 AN INFLECTION LIST PEAK DETECTION ALGORITHM

The algorithm developed is based on a data structure called an inflection list. An **inflection** is a value that is either higher or lower than both the value immediately to the left and the value immediately to the right. If an inflection is higher than its neighbors, it is a **peak**. If it is lower, it is a **valley**. The **inflection list** is a list of all inflections (peaks and valleys) in the data. The idea is to scan the full data set only once to compile a complete list of the inflections. All subsequent scans are of the shorter inflection list, not of the full data set. If the data is "smooth," the inflection list is significantly shorter than the full data set. For our data, the inflection list is typically about 15 % of the length of the full data set. Being smooth is not required for the algorithm to work, but it does significantly decrease processing time.
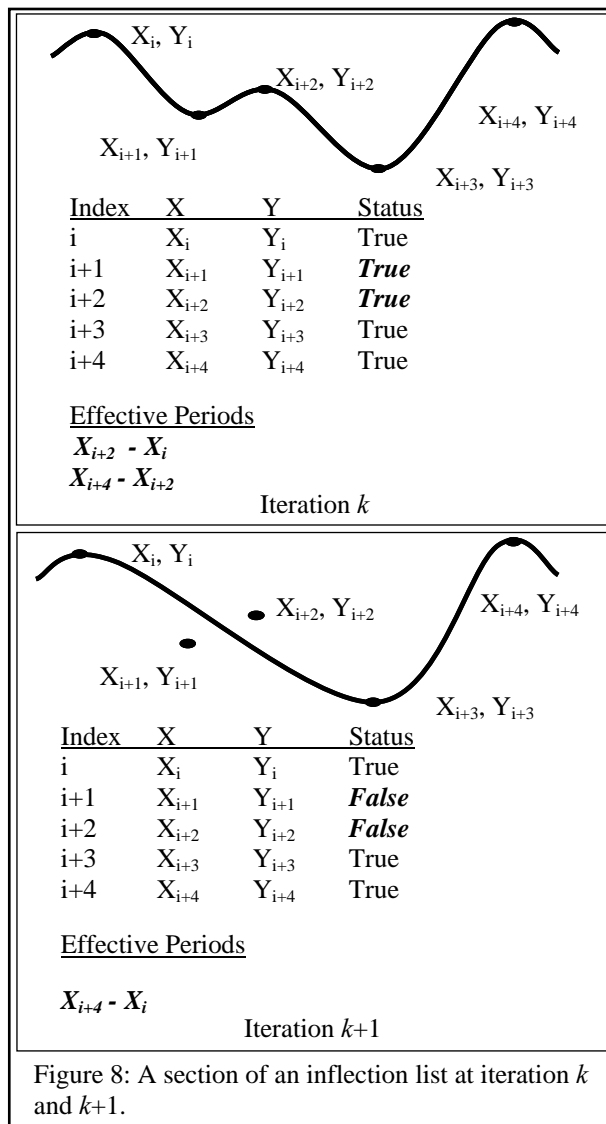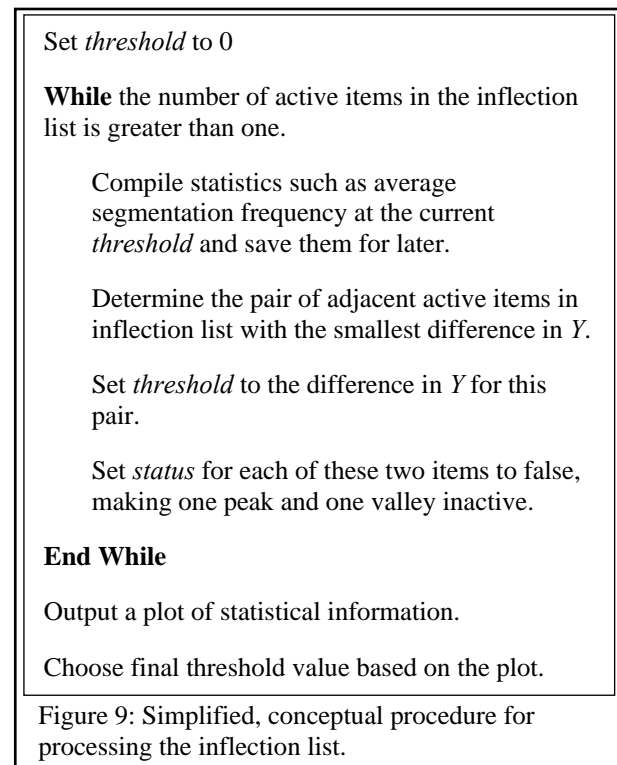

Index	X	Y	Status
i	X_i	Y_i	True
i+1	X_{i+1}	Y_{i+1}	**_True_**
i+2	X_{i+2}	Y_{i+2}	**_True_**
i+3	X_{i+3}	Y_{i+3}	True
i+4	X_{i+4}	Y_{i+4}	True

Effective Periods
$$X_{i+2} - X_i$$
$$X_{i+4} - X_{i+2}$$

Iteration k

Index	X	Y	Status
i	X_i	Y_i	True
i+1	X_{i+1}	Y_{i+1}	**_False_**
i+2	X_{i+2}	Y_{i+2}	**_False_**
i+3	X_{i+3}	Y_{i+3}	True
i+4	X_{i+4}	Y_{i+4}	True

Effective Periods

$$X_{i+4} - X_i$$

Iteration $k+1$

Figure 8: A section of an inflection list at iteration k and $k+1$.

Figure 8 shows example data, a section of the inflection list, and the periods of the peaks at the arbitrary iterations k and $k+1$ of the algorithm. A **period** is the time between two peaks, measured in number of frames. Each entry in the inflection list has three items: The integer X value (frame number), the floating point Y value (*V*), and a Boolean flag called **status**. Status has a value of true if the inflection is **active**, i.e., considered to be significant. Status is false if the inflection is to be ignored. When the inflection list is initially built, all status flags are set to true and the threshold value separating significant and insignificant peaks is set to zero. This indicates that all inflections are initially considered large enough to be significant. As a while loop iterates, the threshold value gradually increases and statistical information on the state of the list at each threshold is compiled until there are no more active inflections. A simplified, conceptual version of this process is shown in Figure 9.

Set *threshold* to 0

While the number of active items in the inflection list is greater than one.

Compile statistics such as average segmentation frequency at the current *threshold* and save them for later.

Determine the pair of adjacent active items in inflection list with the smallest difference in *Y*.

Set *threshold* to the difference in *Y* for this pair.

Set *status* for each of these two items to false, making one peak and one valley inactive.

End While

Output a plot of statistical information.

Choose final threshold value based on the plot.

Figure 9: Simplified, conceptual procedure for processing the inflection list.

The actual program used has minor refinements that improve efficiency. The full program is implemented in a Microsoft Excel macro. Note that the scheme for determining the next threshold is a **minimum consequential step** strategy. If the step size (increase) in the threshold is smaller, there will be no change in the inflection list. If the step size is larger, there may be a loss in resolution of the output plot.

At each iteration k, a histogram of the segmentation periods can be plotted. When comparing the periods for iteration k and $k+1$ in Figure 8, one sees that removing a

peak has the effect of giving the time that peak occupied to a neighboring peak. Thus, two shorter peaks effectively merge into one longer peak. This means that increasing the threshold does not simply truncate the histogram, but also changes its shape.

5 RESULTS AND DISCUSSION

There are three output statistics shown in Figure 10: F_f, the average frequency, defined in Equation 2; F_p, the reciprocal of the average period, defined in Equation 3; and the difference between the two.

$$F_f = \left(\sum_{j=1}^{m} \frac{1}{period_j} \right) \Big/ m \qquad (2)$$

$$F_p = \frac{1}{\left(\sum_{j=1}^{m} period_j \right) \Big/ m} = \frac{m}{\begin{array}{c} length\,of\,time\,from\,start\,of \\ period_1\,to\,end\,of\,period_m \end{array}} \qquad (3)$$
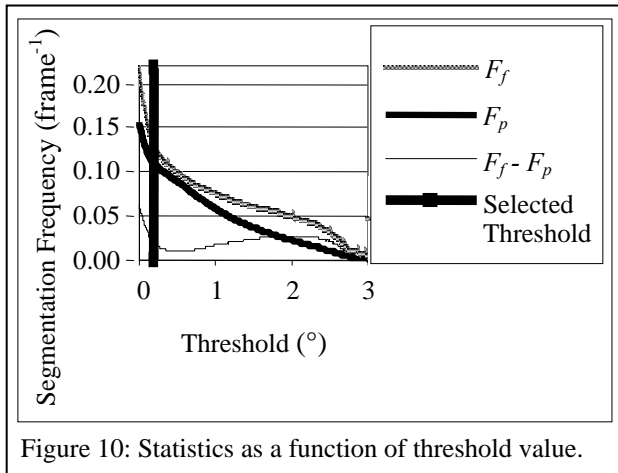

Figure 10: Statistics as a function of threshold value.

The number of segments detected in the movie is designated by m and $period_j$ is the number of frames needed to form segment j. Both F_f and F_p have frequency units (peaks per frame, or cycles per unit of time). For our data, F_f is consistently higher than F_p by at least 10 %. This is important because the machining community compares the segmentation frequencies estimated by different researchers. If the segmentation frequency by one researcher is measured in an F_p manner, and the segmentation frequency from a second researcher is measured in an F_f manner, the two will disagree simply because we are comparing "apples to oranges." Note that it is inherently easier to measure F_p than it is F_f. To measure F_p, one needs only to count the number of segments formed in a given period of time. To measure F_f, the start and stop times of each segment formation must be known.

Both F_f and F_p in Figure 10 drop off steeply for thresholds between 0° and 2°, and less so at thresholds greater than 2°. Several data sets were analyzed and, empirically, the transition from a steep slope to a shallow slope generally yields satisfactory final threshold values when the number of periods is large (well over 1000). However, for some data sets, the change in slope is very small and difficult to detect. In this case, a change in the slope of the difference (F_f - F_p) proved satisfactory. Since a change in the slope of the difference worked in all test cases, it was chosen as the criterion. The precise reason for this behavior is not yet determined. However, some of the factors are briefly discussed in Appendix A.

An advantage of having the plot in Figure 10 is that a simple sensitivity analysis may be quickly performed to assess how sensitive the computed segmentation frequency is to the "error" in the threshold. The sensitivity of the final segmentation frequency output by the algorithm to the threshold value selected by the algorithm is the local slope near the selected threshold. If the slope is steep, the computed segmentation frequency is highly sensitive to the threshold selected. There is less certainty about the quality of the computed segmentation frequency when the slope is steep than when the slope is shallow. However, a method for obtaining the additional information needed to express this as a rigorous uncertainty statement [10] has yet to be determined.

Once a final threshold value has been selected, the plots in Figure 11 are generated. Each plot is a histogram showing the number of occurrences at different segment period lengths. The difference between the two plots is that the horizontal axis is either period for the upper plot or 1/period (frequency) for the lower plot. Vertical bars mark the average period and average frequency.
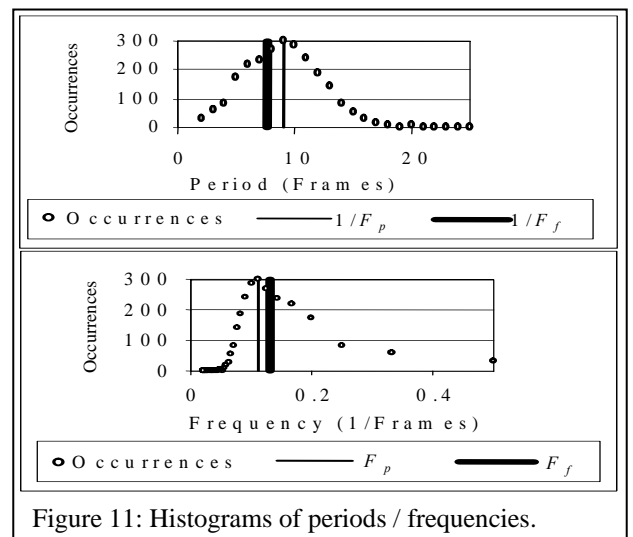

Figure 11: Histograms of periods / frequencies.

From these histograms, further statistical analysis may be performed such as determining variance and skew, and classifying the type of distribution.

Table 1 shows a comparison of segment determinations for two machining movies, each 1000 frames long. One movie imaged "Slow" metal cutting (about 10 frames per segment) and the other imaged "Fast" metal cutting (about 5 frames per segment). For each machining condition, an initial manual determination of segment formation was used as a reference. This reference was compared to both a vector mapping determination ("Vector") and a second manual determination by the same operator on different days ("Manual 2"). Two determinations did not have to occur at exactly the same frame to be considered in agreement; they needed to occur within a few frames of each other to be declared in agreement. When two determinations are compared, they may either be "In Agreement," be a "**False Positive**" (Vector or Manual 2 claimed a segment had formed when the original manual determination claimed that it had not), or be a "**False Negative**" (Vector or Manual 2 claimed a segment had not formed when the original manual determination claimed that it had).

Data Set	Re-measurement Method	In Agreement (%)	False Negative (%)	False Positive (%)
Slow	Vector	93.3	0.0	6.7
Slow	Manual 2	91.9	7.1	1.0
Fast	Vector	86.1	4.3	9.6
Fast	Manual 2	93.5	5.9	0.6

Table 1: Segment determinations for "Slow" (about 10 frames per segment) and "Fast" (about 5 frames per segment) machining conditions.

During both Fast and Slow cutting conditions, the two manual determinations did not agree to better than 94 %. In addition, the Vector determinations consistently claimed more segments existed, as evidenced by the higher False Positive values. Both of these observations may be explained by the phenomenon shown in Figure 7. Many segments do not have obvious spaces between them, making the visual determination of segment formation based on these spaces subjective. The Vector method of segment determination does not require visible spaces between segments. Thus, it seems reasonable that it would detect segments which might be missed by a visual inspection.

The Vector determination agreed with the manual determination under slow cutting conditions (93.3 %) better than under fast cutting conditions (86.1 %). Under fast cutting conditions, there is much more change between adjacent frames in the movie. This increases

errors in the vectors produced by the vector mapping software. Somewhere between 10 and 5 frames per segment, the change in the images from one frame to the next becomes too large for the vector mapping software to determine the vectors accurately. This indicates that one should either set the camera frame rate or machining speed such that at least 10 frames are captured in a typical segment if possible.

6 CONCLUSIONS AND FUTURE WORK

High-speed imaging of machining chips, combined with displacement vector mapping and processing, are powerful techniques to provide valuable chip segmentation data to the machining community. As part of the displacement vector map processing, a novel peak detection algorithm was developed which is efficient, minimizes a priori assumptions about the data, and yields information that assists in uncertainty analysis of the peak detection process. However, further work needs to be performed before a rigorous uncertainty analysis may be completed.

7 ACKNOWLEDGEMENTS

8 REFERENCES

[1] H. Abarbanel, "Analysis of Observed Chaotic Data," Springer-Verlag New York Inc, pp. 1-12, 1996.

[2] J. Barry and G. Byrne, "The Mechanisms of Chip Formation in Machining Hardened Steels," Transactions of the ASME, Volume 124, pp. 528-535, August 2002.

[3] R. Ivester, E. Whitenton, J. Heigel, T. Marushich, C. Arthur, "Measuring Chip Segmentation by High-Speed Microvideography and Comparison to Finite-Element Modeling Simulations," proceedings of the 10th CIRP International Workshop on Modeling of Machining Operations, August 27-28, 2007.

[4] LaVision software "DaVis" and "Strain Master," lavision.de/products/strainmaster.php

[5] National Instruments web site, "Peak Detection using LabVIEW and Measurement Studio," zone.ni.com/devzone/cda/tut/p/id/3770, downloaded 4/13/2007.

[6] T. Park, "Salient Feature Extraction of Musical Instrument Signals" Thesis, Dartmouth College, June 2, 2000.

[7] H. Satar-Boroujeni and B. Shafai, "Peak Tracking and Partial Formation of Music Signals," Proceedings of the 2004 International Conference on

Communications in Computing, CIC '04, Las Vegas, Nevada, pp. 154-159, June 21-24, 2004.

[8] J. Smith III and X. Serra, "PARSHL: An Analysis/Synthesis Program for Non-Harmonic Sounds Based on a Sinusoidal Representation" Proceedings of the International Computer Music Conference, ICMC-87, Tokyo, Computer Music Association, 1987.

[9] Soichi et al. "Peak Detector Using Automatic Threshold Control and Method Therefor," United States Patent 6134279, October 17, 2000.

[10] B. Taylor and C. Kuyatt, "Guidelines for Evaluating and Expressing the Uncertainty of NIST Measurement Results," NIST Technical Note 129, 1994 Edition.

[11] E. Whitenton, R. Ivester, H. Yoon, "Simultaneous Visible and Thermal Imaging of Metals During Machining," Proc. SPIE Vol. 5782, Thermosense XXVII, pp. 71-82, March 2005.

9 APPENDIX A – FACTORS IN THE BEHAVIOR OF F_f - F_p

Figure A1 shows a summary of frequency and period determination equations.

One can model the unimportant peaks as a population of peak heights and widths with some distribution. The important peaks are of a different population and have a different distribution. An appropriate statistic should yield different values for each population. When the algorithm begins, it tentatively assumes all peaks are important by marking them all as active. Thus, at iteration 0, statistics describing the data are the result of the two populations merged together. As the algorithm progresses, it removes the unimportant peaks, one at a time, by marking them as inactive. The population looks less and less like the merged population and more like the population of only important peaks.

The plot in Figure A2 supports this model. The threshold used by the algorithm is plotted as a function of iteration for an actual data set. Initially, the algorithm is removing the small, unimportant peaks and the threshold increases slowly. As the algorithm progresses, there is a point where the threshold starts marking the larger, important peaks as inactive. This causes the threshold to increase at a faster rate due to the difference in population characteristics. The transition occurs at about 1.5°, which is the threshold the algorithm eventually chose. We are investigating using this transition to determine the final threshold in lieu of the current F_f - F_p criteria.

As noted in Section 4, when an active peak is marked as inactive, it effectively yields its time to some other peak. The effect on the statistics describing the remaining population strongly depends on the period of the peak this

time is yielded to. Computer simulations indicate that the F_f - F_p criteria is able to detect if there is a change in the periods of the peaks which are coalescing together.

| Determining the Typical Frequency	Determining the Typical Period
Determine typical frequency by averaging the frequencies f_j: $$F_f = \frac{\sum_{j=1}^{m} f_j}{m}$$	Determine typical period by averaging the frequencies f_j: $$P_f = \frac{1}{\frac{\sum_{j=1}^{m} f_j}{m}} = \frac{1}{\frac{\sum_{j=1}^{m} \frac{1}{p_j}}{m}}$$
Determine typical frequency by averaging the periods p_j: $$F_p = \frac{1}{\frac{\sum_{j=1}^{m} p_j}{m}} = \frac{1}{\frac{\sum_{j=1}^{m} \frac{1}{f_j}}{m}}$$	Determine typical period by averaging the periods p_j: $$P_p = \frac{\sum_{j=1}^{m} p_j}{m}$$
Since F_f is the arithmetic mean and F_p is the harmonic mean of f, $F_f \geq F_p$.	Since P_p is the arithmetic mean and P_f is the harmonic mean of p, $P_p \geq P_f$.

Figure A1: Summary of typical frequency and period determination equations.
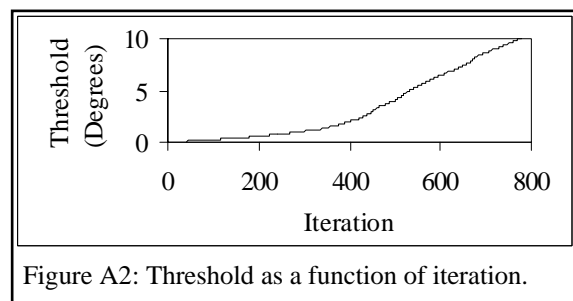
Figure A2: Threshold as a function of iteration.